R. C. Ruchti, et al.

TABLE OF CONTENTS

42 pgs.

A Study of Charm and Beauty Production in Hadronic Interactions

Summary

We propose to extend our measurements of heavy mass particle production in the strong interactions, by using the highest energy beams available at the Tevatron (π^- with $p_{LAB} \geq 600$ GeV/c and protons with $p_{LAB} \geq 800$ GeV/c). The experiment will employ a two-arm spectrometer: an upward muon defining arm to detect prompt muons with laboratory angle $\theta_\mu \geq 40$ mr vertically and momenta $p \geq 5$ GeV/c, and a forward, open-geometry spectrometer to reconstruct the final state.

The yield of heavy mass particles produced by hadron beams is expected to increase substantially at Tevatron. The charm production cross section, modest for present Fermilab energies ($\sigma \approx 20$-40 μb), is expected to improve. Recent upper limits on bare beauty production as well as estimates based on T and ψ production, suggest that $B\bar{B}$ production is very small with presently available beams ($\lesssim 10$ nb/nucleon). However one expects $B\bar{B}$ production to become much more favorable at Tevatron (factor $\gtrsim 5$ larger).

The apparatus will be triggered by several topologies, with a well-defined trigger priority:

(1) prompt muon trigger: This is the principal trigger for the experiment and will be set if one or more minimum-ionizing particles penetrate the length of the upward muon arm.

(2) secondary triggers: (a) high p_T shower trigger - set if an electromagnetic conversion is detected in the liquid Argon calorimeter with $p_T \geq 2$ GeV/c; (b) dimuon trigger-set if two muons are detected in the forward arm, with opening angle consistent with high mass; (c) mass trigger - set if substantial center-of-mass energy is detected well away from the forward direction.

Detection of the associated particles will be provided by a ring-imaging Cerenkov detector to separate π, K in the range $6 \lesssim p \lesssim 30$ GeV/c; a liquid Argon calorimeter for γ, e, π°, η° detection; forward hadron calorimetry and muon detection in a downstream dump; and the fundamental addition of a scintillation counter target to record decays-in-flight of long-lived secondaries ($\tau \geq$ few x 10^{-14} sec).

We will search for heavy mass production by looking for: (i) charm and beauty decays-in-flight (ii) heavy lepton (τ) decays-in-flight (iii) cascade decays b→c (iv) narrow states in weak hadronic decay modes (v) multi-lepton correlations

The experiment should provide $\gtrsim$ 72K detected charm decays per microbarn of cross section, and $\gtrsim$ 120 detected beauty decays per nanobarn in the prompt muon trigger alone.

A total of 1000 hours of Tevatron beam time is requested.

I. Introduction

In the fall of 1974 the discovery of the J/ψ at Brookhaven and SLAC heralded the production of hadrons containing new constituents. An immediate implication of the J/ψ (interpreted as a bound state of charm-anticharm quarks) was that a large family of related "bare" charm particles should exist. Since 1976, the spectroscopy of these particles has unfolded dramatically, with the observation of numerous charmed mesons and several charmed baryons. A systematic study of the charm system, including analysis of observed states and searches for as yet unobserved states and decay modes, is in progress at several laboratories. One of these experiments, Fermilab E515[1], is a comprehensive survey of charm particle production in 200 GeV/c π^- - Be collisions utilizing a prompt muon trigger.

Although the spectroscopy of charm mesons (D,D*) has been well studied in e^+e^- annihilations, those machines have, to date, not provided comparable measurements of the spectroscopy of charm baryons or the more exotic charm states such as F mesons. In addition, the nature of hadronic charm production, and more generally the hadronic pair-production of heavy mass particles, is essentially unknown. Specifically the hadro-production of heavy quark masses should be important in the further understanding of QCD. Lastly, lifetimes of charm particles will, most likely, be measured only in fixed target experiments.

Tevatron energy beams should enhance the study of charm in several ways: the increased center-of-mass energy will admit to larger, more favorable production cross sections, ($\sigma_{c\bar{c}} \geq 50$ μb) and to longer mean decay lengths for decays-in-flight of charm particles.

The discovery of the T at Fermilab[2] in 1977 indicated the existence of yet another quark system. One naturally expects that there should exist a familial arrangement of beauty quarks in combination with well-known (u, d, s, c) quarks, in analogy to the charm system. Preliminary results from CESR indicate that bare beauty particles are being produced in e^+e^- annihilations in the T(10550) mass region[3].

One's ability to observe beauty states depends, of course, on the production cross section at a given center-of-mass energy and branching ratios for b decay. Experimental measurements indicate that the cross section for upsilon production in 400 GeV/c nucleon-nucleon collisions is very small:[2]

$$B_{\mu\mu}\left(\frac{d\sigma}{dy}\right)_{y=0} = 0.3 \times 10^{-36}\ \text{cm}^2/\text{nucleon}.$$

This cross section is well below the sensitivity range of most experiments other than those triggering on dileptons. However the prospects for "bare" beauty production may not be as bleak as the cross sections for upsilon production by protons might indicate.

(i) Several recent experiments have set limits on hadronic

$B\bar{B}$ production by looking for events with three muons in the final state. The 3μ events are assumed to originate from either of two topologies,

$$\pi(\text{or } p) + N \rightarrow B_1 + \bar{B}_2 + X \qquad (1)$$
$$B_1 \rightarrow \mu$$
$$\bar{B}_2 \rightarrow \psi$$
$$\psi \rightarrow \mu^+\mu^-$$

$$\pi + N \rightarrow B_1 + \bar{B}_2 + X \qquad (2)$$
$$B_1 \rightarrow \mu$$
$$\bar{B}_2 \rightarrow \bar{C} + \mu$$
$$\bar{C} \rightarrow \mu$$

(where we denote any beauty particle, meson or baryon, by B). The inferred production limits are $\sigma_{B\bar{B}} \lesssim 7.5\text{-}50$ nb for reaction (1)[4,5,6], and $\sigma_{B\bar{B}} \lesssim 25\text{-}100$ nb for reaction (2)[7]. These results involve model dependent p_T cuts on the (non-T) muons as well as branching ratio assumptions.

(ii) One can also estimate the level of $B\bar{B}$ production by scaling from T production.

(a) Upsilon production by pions[8] is more effective than production by protons at $\sqrt{s} = 23$. It is reasonable to assume that a similar advantage exists for $B\bar{B}$ production, and hence a pion beam would be preferable for a first experiment.

(b) The ratio of the cross sections for producing pairs of "bare" particles to inclusive production of the related vector meson is large and appears to

increase with increasing constituent mass. For example the ratio:

$$\frac{\sigma_{K\bar{K}}}{\sigma_{\phi}} \simeq 20 \text{ at Fermilab energies}^{9}$$

whereas

$$\frac{\sigma_{D\bar{D}}}{\sigma_{J/\Psi}} \simeq 100 \text{ in the same energy regime}^{10}.$$

One might then expect a similar gain from charm to beauty:

$$\frac{\sigma_{B\bar{B}}}{\sigma_{\Upsilon}} \gtrsim \frac{\sigma_{D\bar{D}}}{\sigma_{J/\Psi}}$$

If one then looks for beauty production in $\pi^{-}N$ interactions one obtains the following estimate for the production cross section

$$\sigma_{\pi N \to B\bar{B}X} \simeq \left(\frac{\sigma_{B\bar{B}}}{\sigma_{T}}\right)\left(\frac{\Delta y}{B_{\mu\mu}}\right)\left(B_{\mu\mu}\,\frac{d\sigma}{dy}\right)_{y=0;\ \pi N \to TX \hookrightarrow \mu\mu}$$

$$= (100) \times \frac{2}{.035} \times (1.5 \times 10^{-36}) \ \text{cm}^2/\text{nucleon}$$

$$\simeq 10 \text{ nb/nucleon} \quad ; \quad \text{assuming 200 GeV/c beam } (\sqrt{s} \simeq 19 \text{ Gev}) \text{ and } B(d\sigma/dy) \text{ value to be that from ref. 8}$$

This result is comparable to the experimental upper limits described above.

One can then infer what the cross section will be for higher energy beams by scaling from the ψ to Υ systems[11] (see fig. 1). Assuming that the ψ and Υ cross sections behave similarly as a function of $\tau=M^2/s$, one can expect a factor of $\gtrsim$5 gain in cross section using 600 GeV/c pions rather than 200 GeV/c pions. This suggests

$$\sigma_{\pi N \to B\bar{B}X} \simeq 50 \text{ nb/nucleon (for } \begin{matrix} 600 \text{ GeV/c pions} \\ \sqrt{s} = 33.6 \end{matrix}$$

(iii) Estimates of hadronic beauty production based on Fusion Models indicate similar cross sections for $pp \to B\bar{B}X$.[12]

Depending upon the cross section levels observed, one can anticipate making a number of important measurements using an open geometry spectrometer and an active target:

(a) if $\sigma_{B\bar{B}} \gtrsim 1$nb, one can establish the production level, and measure B particle lifetimes. Observation of chain decays will indicate relative strengths of $b \to c$ vs $b \to u$.

(b) if $\sigma_{B\bar{B}} \gtrsim 10$nb, precision lifetime measurements are possible, production distributions will be available, and a (limited) spectroscopy might ensue.

(c) if $\sigma_{B\bar{B}} \gtrsim 50$nb, substantive spectroscopy of the $B\bar{B}$ system may be possible.

Finally, an important component of F meson decay (and to some extent B decay) should be τ lepton. These decays should also be recorded in an active target, including the channels $\tau \to \rho\nu$, $\mu\nu\bar{\nu}$, $e\nu\bar{\nu}$.[13] Measurement of the τ lifetime is important because it is a calculable quantity. In addition, pair production and subsequent decay of any new leptons which are long-lived, and which decay to muons, or electrons should be observable.

We intend to improve our cross section sensitivity substantially (over E515) for decays of heavy high mass particles produced in π^- and proton induced reactions. First, we will replace the existing Be target with an active, scintillator target to record decays-in-flight. Second, a shortened and more powerful Cerenkov counter (ring imaging) will be used for π and K separation in the momentum range 6 - 30 GeV/c. Third, neutral detection will be enhanced by a substantial increase in solid angle coverage and by the implementation of a new shower detector lattice. Fourth, forward muon coverage will be expanded by a factor of two in a downstream dump. The dump will also be instrumented for hadron calorimetry. The magnetic spectrometer currently existing for E-515, will be retained intact. (See figure 2 for a comparison of the geometry of this experiment versus E-515, and appendix I for hardware details).

The experimental apparatus will be triggered in several ways. The primary trigger is a muon detected in the upper arm ($\theta \gtrsim 40$ mr vertically) in conjunction with a positive signal in the forward arm. Additionally, there will be secondary triggers including: an electromagnetic shower detected in the liquid Argon detector with $p_T \gtrsim 2$ GeV/c; a forward multi-lepton trigger; and a dimuon trigger optimized to $\psi \to \mu\mu$ for calibration purposes.

We will require a beam flux of $\gtrsim 5 \times 10^7$ particles per pulse with spot requirements identical to E-515. We intend to run with both a π^- beam ($p_{LAB} \gtrsim 600$ GeV/c) and protons ($p_{LAB} \gtrsim 800$ GeV/c). Assuming 1000 hours of beam time for data taking, we expect a yield of $\gtrsim 120$ detected B decays-in-flight per nanobarn of cross section in events triggered by a prompt muon.

II. Experimental Strategy

The reaction to be investigated is:

$$\pi^-(\text{or } p) + N \to P_1 + \bar{P}_2 + X$$

P_1 → (Trigger Particle)

$\bar{P}_2 \to D\bar{D}K$, $K\pi$, etc.

where $P_{1,2}$ represent charm or beauty particles. Our strategy will be to search for high mass particle production in the strong interactions using several trigger techniques.

(1) Prompt Muon Trigger

The apparatus will be triggered, principally, by the detection of a prompt muon from the target, a method with which we have long-standing experience (E397, E515)[1]. The advantage here is that we trigger on a muon from the semi-leptonic decay of one particle, $\theta_{\mu}^{LAB} \gtrsim 40$ mr vertically, and look for the decay of the associated particle in a separate, large-acceptance arm. A possible decay topology is:

$$\pi^-(\text{or } p) + N \rightarrow B_1 + \bar{B}_2 + X$$
$$\bar{B}_2 \hookrightarrow \mu^+ + X$$
$$B_1 \hookrightarrow D^0\bar{D}^0K$$
$$\text{or } B_1 \hookrightarrow D\pi$$
$$\text{or } B_1 \hookrightarrow \psi K\pi, \quad \psi \hookrightarrow e^+e^-$$

where the μ^+ from $\bar{B}_2$ decay (trigger muon) is observed in the upward arm. The decay of the associated state (B_1) is detected in the forward arm, which is instrumented with Cerenkov, shower, and muon detectors to identify the decay products. The B_1 mass is then kinematically reconstructed with a resolution $\frac{\delta m}{m} \sim 1\%$.

It is important to note that the prompt muon trigger allows us to examine, in an unbiased way, the decay channels of these particles - mesons or baryons. This is crucial for

branching ratio measurements, and pair production studies. Also of interest is the correlation between the charge of the muon in the trigger arm and the sign of charged kaons in the forward arm as a function of p_T for the trigger muon. For example, in charm decays, the $\Delta C = \Delta Q$ rule requires that the charge of the trigger muon be of the same sign as the sign of the charged kaon from the decay of the associated particle:

$$\pi^-(\text{or } p) + N \rightarrow D_1 + \bar{D}_2 + X$$
$$\qquad\qquad\qquad\qquad\quad \hookrightarrow \mu^- + X$$
$$\qquad\qquad\qquad\qquad\quad \hookrightarrow K^-\pi^+ \quad (K^+\pi^- \text{ not allowed})^{14}$$

This correlation should dominate for transverse momenta $p_T \lesssim$ 1 GeV/c. For Beauty decays, one expects the opposite case (for muons coming directly from B rather than from subsequent charm decays):

$$\pi^-(\text{or } p) + N \rightarrow B_1 + \bar{B}_2 + X$$
$$\qquad\qquad\qquad\qquad\quad \hookrightarrow \mu^+ + X$$
$$\qquad\qquad\qquad\qquad\quad \hookrightarrow C_1 + X$$
$$\qquad\qquad\qquad\qquad\qquad\quad \hookrightarrow K^-\pi^+ \quad (\text{not } K^+\pi^-)$$

This correlation should dominate at larger p_T ($\gtrsim$1.5 GeV/c). Lack of such a correlation in $B^0\bar{B}^0$ systems would indicate $B\bar{B}$ mixing.

For Beauty, the yield of events in any individual hadronic, weak decay mode will be small (for details see section III). However the approach should still be tractable because the active target will allow us to associate the downstream tracking with the appropriate decay vertex, minimizing combinatorial difficulties. The wealth of potential decay channels makes this approach both appealing and compelling.

Trigger rates for the prompt muon trigger should be $\sim$50% of those for E-515 because of the larger $\langle p_T \rangle$ requirement for the trigger muons. We expect $\sim 10^{-5}$ triggers per interaction. Assuming 5×10^7 π^-/minute and a 10% target, this yields 50 triggers/minute. Based on preliminary results from E-515, $\geq$40% of these triggers will yield a trackable muon in the upward arm; of these, $\sim$25% should be associable to weak decay.

(2) Secondary Triggers:

(a) High p_T Shower Trigger: This trigger will be formed by requiring a large energy deposition in the shower detector, at a vertical angle consistent with large p_T. In addition to B decays which will produce electrons at large p_T, both ψ and Υ decays should contribute significantly. A trigger set at $p_T \geq 2$ GeV/c will provide good efficiency for detecting B, ψ, and Υ decays; low mass systems will be strongly suppressed.

Trigger rates for this mode will be controlled by the p_T cut, which will be adjusted to yield $\sim 10^{-5}$ triggers per interaction (comparable to the prompt muon rate).

(b) Multi-lepton Trigger: This trigger, which requires three leptons in the forward arm of the apparatus, emphasizes $B\bar{B}$ pair production as indicated below:

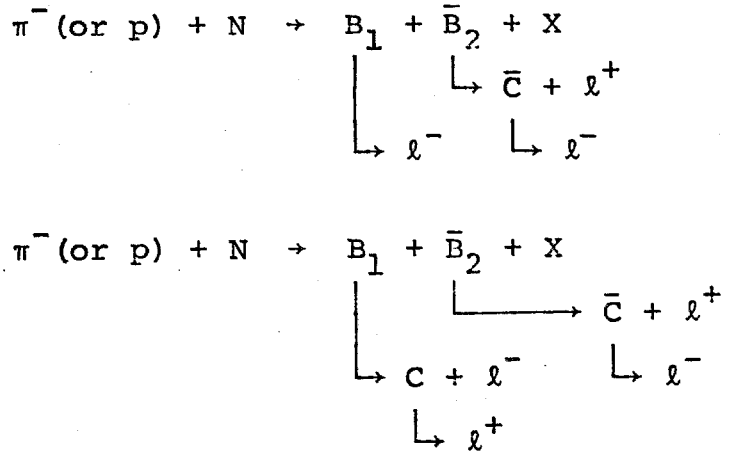

It is expected that the trigger rate for three lepton events (combinations of μ and e) will be exceedingly low. Nevertheless these events should yield a very clean sample of B decays in the active target.

(c) Dimuon Trigger: This trigger, suitably prescaled, will be used to calibrate the spectrometer using $\psi \to \mu^+\mu^-$ decays.

(d) Mass Trigger: A more speculative, yet interesting, possibility is to trigger on a substantial fraction of center-of-mass energy away from the central region near the beam. Such a trigger could be effected using the shower

detector and/or a suitably instrumented forward hadron calorimeter (instrumentation within the forward dump). A substantial fraction of such events could contain high mass particles.

III. Event Yields

Event yields are calculated for a run of 1000 hours, assuming 5×10^7 beam particles/minute, a 10% interaction target, and a 66% duty factor. This translates into 2×10^{11} interactions in the active target. The yield of events per nanobarn of cross sections is then:

$$\text{Yield/nb} = \frac{2 \times 10^{11}}{20 \text{ mb}} \times 1.0 \text{ nb} = 10^4$$

The actual yields into any specific decay topology will depend on the appropriate branching ratios (BR) and acceptance (A).

1. Beauty Production (refer to Table I)

   Assuming 50 nb/nucleon of beauty production at 600 GeV/c, we expect to observe:

   a) In association with a prompt muon in the upward arm:

      i) 125 hadronic weak decays of associated B particles

      ii) 750 semi-leptonic decays (into μ or e) of the associated B particle, including:

      100 three lepton events ($\mu \ell_1 \ell_2$, where $\ell_{1,2}$ are μ or e and $\Sigma Q_\ell = \pm 1$, where Q_ℓ's are lepton charges)

5 four lepton events ($\mu\ell_1\ell_2\ell_3$, where $\ell_{1,2,3}$ are μ or e and $\Sigma Q_\ell^{1,2,3}=0$ where Q_ℓ are lepton charges)

b) The multi-lepton trigger is expected to contribute:

i) 1000 three lepton events ($\ell\ell\ell$ and $\Sigma Q_\ell = \pm 1$)

ii) 125 four lepton events ($\ell\ell\ell\ell$ and $\Sigma Q_\ell = 0$)

We expect the multi-lepton events to yield a clean sample of B and $\bar{B}$ decays. To assess how well one might do in search of weak hadronic decays of beauty particles, we note that recent results from CESR[3] indicate that the mean charge multiplicity observed in the T(10550) region is $\sim$12 (or 6 charged secondaries per B decay). One expects an additional $3\pi^\circ$ per B decay as well.

The ability to isolate B decays in the active target should reduce the combinatorial background in mass plots by a large factor over what it would be without vertex information.[15] However our ability to identify unique hadronic modes will depend critically upon branching ratios into readily identifiable channels.

2. Charm Production (Refer to Table II)

Assuming 50 μb/nucleon of charm production at 600 GeV/c, we expect to observe:

in association with a prompt muon in the upward arm:

i) 270K hadronic weak decays of charm particles

ii) 450K semi-leptonic decays (into μ or e) of charm particles

Combinatorial backgrounds in hadronic weak decay channels for charm particles will be minimal for decays involving all-charged secondaries. For decays containing neutrals, the combinatorial suppression will be even stronger than in the Beauty case because of the substantially lower average multiplicity in the decays.

IV. Conclusion

We feel that the prompt muon trigger is a unique tool for the study of weak decays of high mass states: first for its experimental simplicity, and second for its power to select rare processes from a substantial hadronic background.

By employing this trigger (and others) in conjunction with a sophisticated, open geometry spectrometer and active target system, we feel that this experiment will be a definitive probe of charm and beauty and of the nature of the strong interactions.

We request 1000 hours for our studies.

V. References

1. Fermilab Experiment 515: A Search for Charm Particles Produced in Hadronic Interactions, Northwestern-Carnegie Mellon-Notre Dame-Fermilab Collaboration. First data for this experiment was recorded in Spring 1980. A second run will occur in Spring 1981.
2. S. W. Herb, et al., Phys. Rev. Lett. 39, 252 (1977); and W. Innes, et al., Phys. Rev. Lett. 39, 1240 (1977) , K. Ueno, et al., Phys. Rev. Lett. 42,486(1979).
3. E. H. Thorndike, "First Results on Bare b Physics", Talk given at the XXth International Conference on High Energy Physics, Madison, Wisconsin, July 17-23, 1980; and G. Moneti, "Results from CESR", HEPSY Memo 15-80, SLAC Summer Institute, August, 1980.
4. J. Badier, et al., CERN/EP 80-89 (4 June 1980)
5. A. Diamant-Berger, et al ., Phys. Rev. Lett. 44, 507(1980).
6. P. Musset, CERN/EP 80-161 (27 August 1980)
7. R. N. Coleman, et al. C00-3072-105 (Fermilab CIP Collaboration); and reference 6.
8. J. Badier, et al., CERN/EP 79-88 (August, 1979); J. Badier, et al., CERN/EP 80-149 (13 August 1979)
9. K. J. Anderson, et al., Phys. Rev. Lett. 37, 799 (1976); and V. Blobel, et al., Phys. Lett. 59B, 88 (1975)
10. Based on $\sigma_T(J/\psi) = \frac{2}{B_{\mu\mu}} (B \frac{d\sigma}{dy})_{y=0} = 280$ nb/nucleon for pions of 200 GeV/c momentum, and $\sigma_{c\bar{c}} \simeq 25$ μb/nucleon in the same energy range.
11. Data from J. Badier, et al., CERN/EP 80-149 (13 August 1979) and references listed therein.

V. References

12. See proceedings of the Tevatron Workshop (1980); unpublished.

13. The decay $\tau \rightarrow \rho\nu$ is a very interesting mode for several reasons: it has a large branching ratio ($\simeq$20%); it is a two-body decay; and it will appear (topologically) in the target as a charged track with a single kink. Assuming the $\rho^{\pm} \rightarrow \pi^{\pm}\pi^{0}$ can be reconstructed, the γ for the parent can be determined if m_{τ} = 1790 is assumed.

14. This assumes that D^{0}, $\overline{D^{0}}$ mixing is negligible.

15. Combinatorial backgrounds in mass plots will not be completely suppressed even with the use of an active target because of neutral secondaries (π^{0},η^{0},K^{0},Λ^{0}) associated with decay vertices.

Table I : Beauty (per nb of cross section)

Prompt Muon Trigger:

		A	BR	Yield/nb	Vertex Detected
Trigger:	$B_1 \rightarrow \mu$	2 x 5%	12%	120	120
	$B_2 \rightarrow \mu,e$	50%	25%	15	15
	$B_2 \rightarrow$ hadrons	5%	75%	5	2.5
	μll (3 Leptons)	25%	6.3%	2	2
	μlll (4 Leptons)	6.3%	1.6%	0.1	0.1

Multimuon Trigger:

$B_1 \rightarrow 2\ell$, $B_2 \rightarrow \ell$	12.5%	1.6%	20	20
$B_2 \rightarrow 2\ell$	6.3%	0.4%	2.5	2.5

Table II: Charm (per μb of cross section)

Prompt muon trigger:

		A	BR	Yield/μb	Vertex Detected
Trigger:	$C_1 \rightarrow \mu$	2 x 3.0%	12%	72K	72K
	$C_2 \rightarrow \mu,e$	50%	25%	9K	9K
	$C_2 \rightarrow$ hadrons	20%	75%	10.8K	5.4K

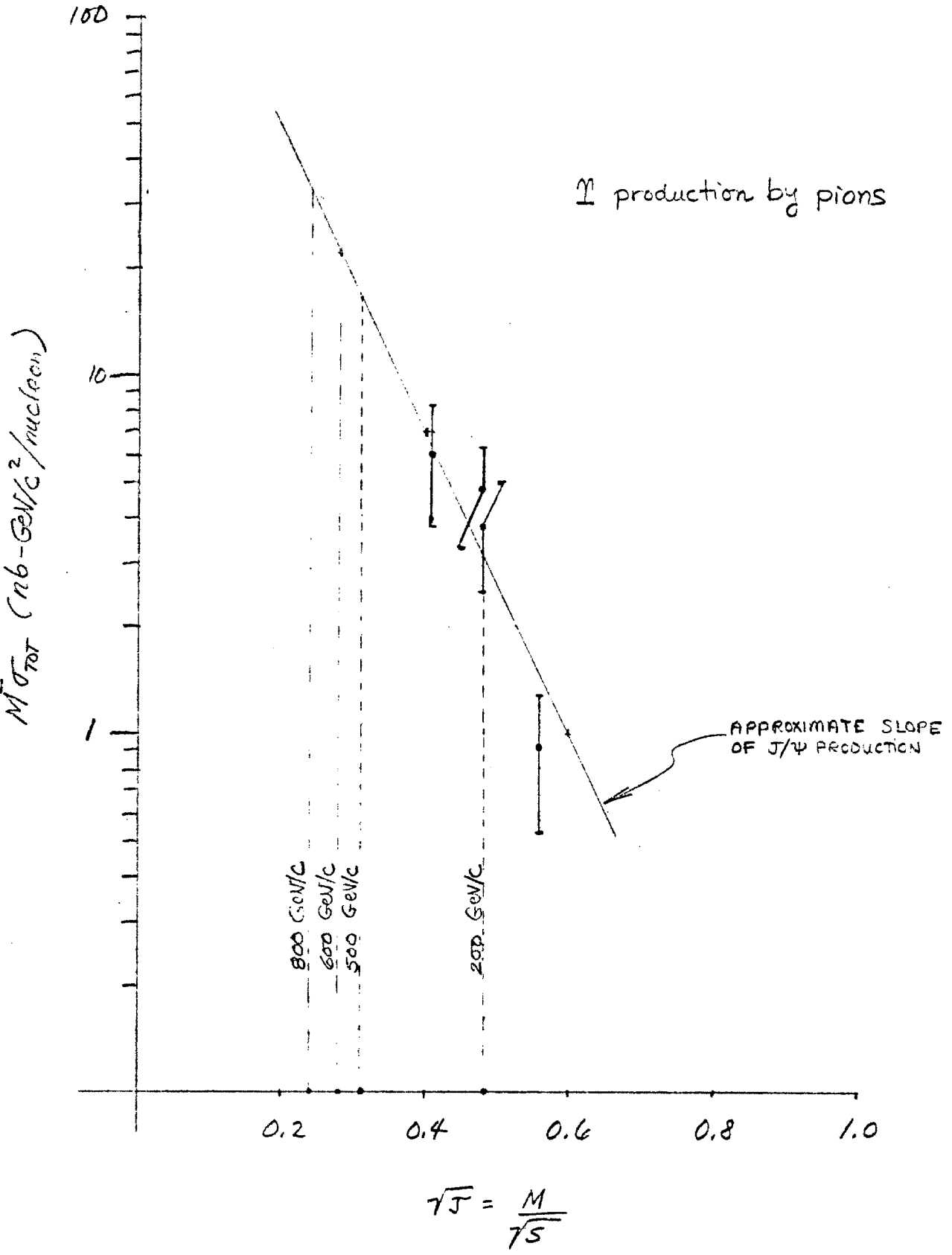

Fig. 1 RECENT DATA ON PION INDUCED UPSILON PRODUCTION. (see ref. 11)

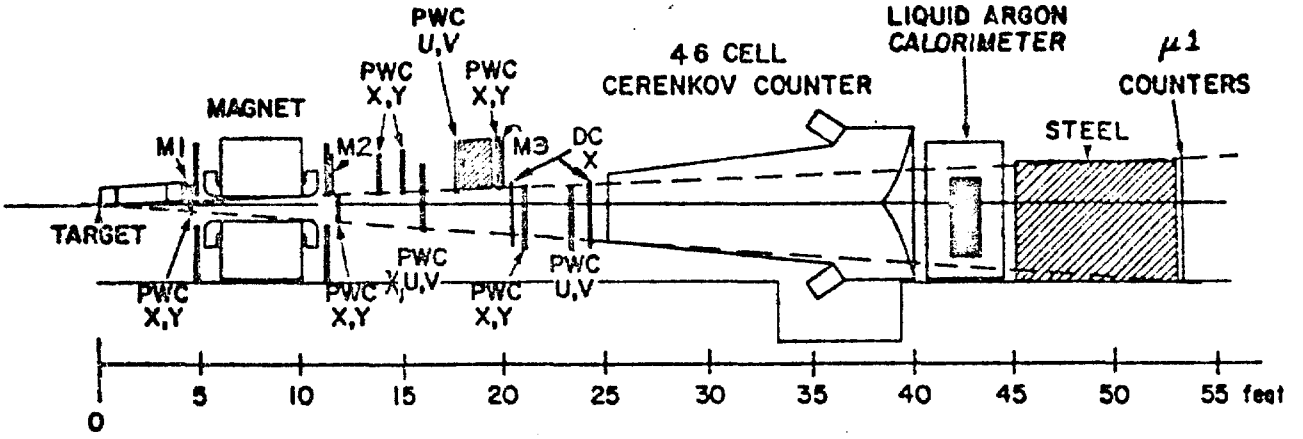

E515 ELEVATION VIEW

Fig. 2a

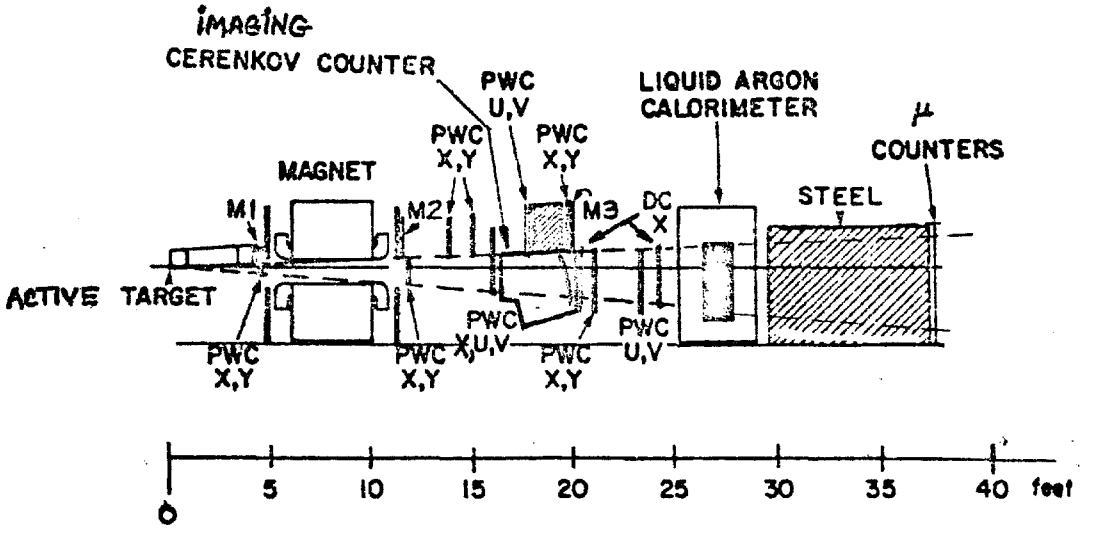

Fig. 2b Elevation view for this proposal

Appendix I: Hardware Development

A study of charm production in the strong interactions is feasible using a passive target and downstream detector system; however that technique is insufficient for a beauty search. The expected small beauty cross section ($\sigma_{B\bar{B}} \simeq$ 50 nb) and the high multiplicity expected for B decays require a new experimental strategy. To meet the demands of beauty physics, we intend to augment the E-515 apparatus with three new detectors, and to redeploy some existing equipment (see Fig. 2b). The magnetic spectrometer will remain intact. The present Be target will be replaced by an active, scintillation target allowing us to observe decays in flight of particles produced in the primary interaction. This device will not only allow us to measure particle lifetimes, but will minimize combinatorial background problems in the reconstruction of particle masses. The existing Cerenkov counter will be replaced by a (1 m long) imaging Cerenkov system. Last, a new liquid Argon shower detector will be constructed with a lattice optimized to a much reduced target-to-shower-detector distance. The new Cerenkov and shower systems will substantially increase our ability to unambiguously reconstruct the decays of high mass systems, in the face of attendant high multiplicity.

1. Active Target. The appropriate choice of target to be used with our spectrometer system is dictated by the following objectives:

i) for trigger purposes, the target must be compatible with our present beam/target geometry (an essential point to minimize π, K decay background in the muon trigger).

ii) the target must be able to survive and operate in a high flux environment (in the range $> 10^6$ interactions/sec. over long periods).

iii) excellent spatial resolution is required ($\sim 15\,\mu$).

iv) the number of individual measurements per unit track length should be sufficient to observe decays in flight ($\sim$ 50 μ between "hits" is a useful working number).

v) response time should be fast and dead time minimal in order to have a useful duty factor.

All these objectives are nicely accommodated through the use of a scintillation target, for which the active element is a NaI or CaI_2 crystal (typical dimensions 2 cm x 2 cm x 0.5 mm). Preliminary work on scintillation camera techniques (see Appendix I) has been performed by D. Potter. The scintillation light produced in the crystal target is collected through a specially matched lens onto an image intensifier. By gating a stage of the image intensifier with the trigger logic, one can selectively record triggers on film. It is interesting to note that of the two target crystals, CaI_2 is superior to NaI as a scintillant ($\sim$ a factor 2 in light yield). Unfortunately its monoclinic (mica-like) crystal structure has precluded its use in large crystal arrays. However, for our application such a crystal structure poses no problem, since the crystal will be very thin in vertical dimension (0.5 mm). Based on the preliminary studies we anticipate $\sim 10\,\mu$ spatial resolution per detected photon and 8-10 detected photons/mm using a NaI target; CaI_2 should double the light yield (16-20 photons/mm) without degrading the spatial resolution. These targets will undergo preliminary

tests with the E-515 apparatus at the end of the forthcoming spring 1981 run. During this period we will be looking for charm decays using the scintillation camera system.

A limitation of these targets is the number of detected photons per mm of track length (corresponding to 50-100 μ between successive "hits"). This difficulty can be surmounted through the use of a microchannel plate target (preliminary results are reported in Appendix II), or matrix target consisting of individual, optically-isolated crystals of NaI (dimensions 15 μ x 15 μ x 0.5 mm) arrayed to form a composite target of overall dimension 2 cm x 2 cm x 0.5 mm (see Fig.A1). It is known that NaI produces 20K photons per millimeter of minimum ionizing track. Hence ~ 200 photons will be generated per scintillation element per track. Clearly not all of the photons will emerge from the end of an element since losses will occur over multiple internal reflections. Given a refractive index of n~1.8 for NaI,light produced at the far end of a crystal would require roughly 50 internal reflections to traverse 0.5 mm. Assuming a (reasonable) reflectivity of ~ 93% at each boundary encounter, a minimum of 5 photons (worst case) would emerge from the end of the scintillator. This signal can be first preamplified in a microchannel plate, or coupled directly to an image intensifier or photo diode array. The key point is that a matrix target(either scintillation fibers or michrochannel plate) would allow us to avoid the use of a lens system with its attendant high light loss due to finite(and small) angular acceptance.

Preliminary tests by Harshaw Chemical Company are required to establish the fabrication techniques for making small scintillation fibers. Should the tests prove successful, we plan to incorporate the matrix target into the spectrometer.

Ultimately the limitation of the matrix target device, as presently envisaged, is camera speed (> 15 msec.). We have considered numerous alternatives to film, including channeltron photomultiplier tubes, vidicon systems, etc., but either the readout is too slow or spatial resolution is considerably degraded. To our knowledge, film currently provides the best means of preserving the target resolution with at least a "reasonable" duty factor. Notre Dame is equipped with four measuring machines (soon to be interfaced to a VAX computer system), and Rutgers has a PEPR system, so film analysis capability exists. Nevertheless, we will continue to explore all-electronic readout options. Using the scintillation target, we expect to measure particle mean lifetimes of order $\gtrsim 10^{-14}$ sec.

2. Imaging Cerenkov Counter. The motivation for implementing an imaging Cerenkov system is based on the following criteria:

i) the need for optimal pattern recognition capability in the face of high multiplicity ($< n > \sim 6$-10) events.

ii) the need for π and K separation over an extensive momentum range $5 \lesssim p \lesssim 30$ GeV/c in a single counter.

iii) the need for maximum acceptance for other detectors necessarily situated downstream (particularly the liquid argon shower detector). This implies the shortest possible radiator length in the Cerenkov system consistent with good photostatistics.

The development of the avalanche chamber[1](which utilizes, as its gas mixture, a UV-sensitive photoionizing gas in conjunction with an inert gas) has provided a means for detecting not only Cerenkov light, but also its spatial character.

A schematic of 1/4 of the detector is shown in Fig. A2. Particles of sufficient velocity ($P_\pi > 6$ GeV/c, $P_K > 20$ GeV/c) will radiate in the meter-long, atmospheric pressure, N_2 gas counter. The Cerenkov light is imaged by a spherical mirror onto an avalanche chamber, placed approximately at the focal plane of the mirror. The detector and its working gas mixture are physically isolated yet optically coupled to the N_2 gas radiator volume by a LiF window (in reality a mosaic of six crystals, each 5 cm x 20 cm x 2 mm in size, arrayed to form a rectangular window of cross sectional dimensions 30 cm x 20 cm, and 2 mm thickness).

We intend to use, at the outset, an admixture of 5% triethylamine (TEA) in argon as the working gas mixture for the avalanche chamber. Photoionization of TEA is most favorable for UV light at 1500 Å. The LiF crystals transmit light down to ~1100 Å and hence will pass wavelengths of interest ($\gtrsim$80% transmission). Also the reflective coatings on the spherical mirrors will be optimized for 1500 Å by overcoating the aluminum with the appropriate thickness of MgF_2.

The Cerenkov angle for particles well above threshold in the N_2 radiator is ~ 25 mrad. Since our spherical mirrors are of 2 meter radius, this results in a ring-image diameter of 5 cm at the avalanche detector planes. In fact the images are somewhat elliptical, since the true focal surface is non-planar.

The ring image is detected using x, u, v wires in the proportional chamber end of the avalanche chamber (see Fig. A3). Preliminary tests with an ^{55}Fe X-ray source have yielded large, proportional pulses in the Argon/TEA mixture. Expected signal sizes (into 50 Ω) in the working detector are

$\sim 50\ \mu V$ per anode (x) wire and $\sim 25\ \mu V$ per cathode (u and v) wire, for each converted photon in the chamber. Our front-end amplifier (LeCroy TRA401) can handle such signals adequately. We expect to detect ≥ 6 photon conversions per particle well above threshold based on recent data from a CERN group.[2]

A test cell, including all critical detector components, will be operated in the M1 beam at Fermilab during early 1981. Pending the outcome of the initial testing, the detector itself may be incorporated into the E-515 geometry during the spring 1981 data run of that experiment.

For the beauty search experiment, we plan to replace the sagged-glass spherical mirrors presently being used with parabolic mirrors, to generate (effectively) a planar focal surface. We should then obtain crisp circular images on the detector planes. Ultimately this counter should provide π K separation in the momentum range $5 \lesssim p \lesssim 30$ GeV/c using photon counting and ring-imaging techniques.

3. Shower Detector. A new 4' x 8' liquid Argon Shower detector will be constructed (a portion of one quadrant is shown in Fig. A4). The beam will pass through a 12" diameter hole at the center. The central region from 6" < R < 12" will be instrumented with a core detector comprised of alternating layers of u,v readout strips (128 u channels, 128 v channels). This strip configuration was chosen to maximize the orthogonality of the u,v coordinate measurements and to minimize the number of v strips that a given u strip will overlap (and vice-versa). The resultant lattice should help to minimize pattern recognition problems in the central region of the overall detector where the number of showers is maximal. The outer quadrants (R > 12")

are well decoupled from the beam region and will be used for triggering. Instrumentation here will consist of alternating layers of x,y readout strips - a coordinate system which is readily amenable to p_T and energy moment (mass) triggering. The detector will also be subdivided longitudinally into upstream and downstream halves, to assist in the separation of electromagnetic showers from hadronic showers.

The acceptance of the detector in terms of $(x,x_\perp)$ is shown in figure A5, assuming a 600 GeV/c beam of pions ($\gamma \simeq 17$). It is important to note that conventional (and undesirable) backgrounds are confined to small $x_\perp$ values and lie near the horizontal axis. Of these, approximately 1% or less will fall into our acceptance.

References

1. G. Charpak and F. Sauli, Phys. Lett. 78B, 523 (1978);

G. Charpak, et al., Nuc. Instr. and Meth. 164, 419 (1979).

2. J. Seguinot, et al., Nuc. Instr. and Meth. 173, 283 (1980).

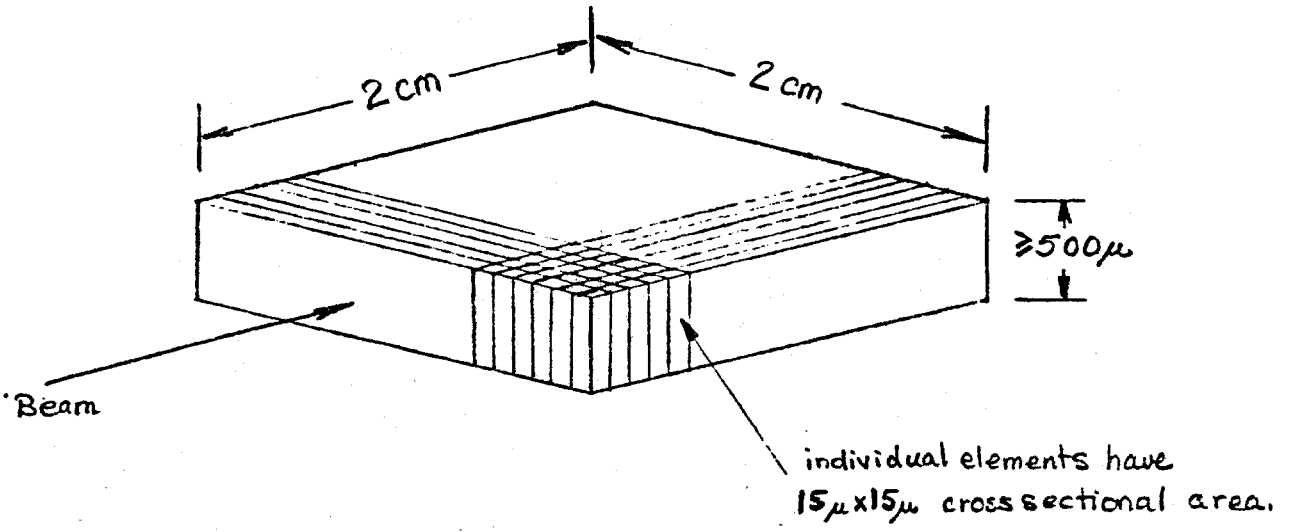

Fig. A1 Schematic of Matrix Target, Indicating Some of the Small NaI Scintillation Elements.

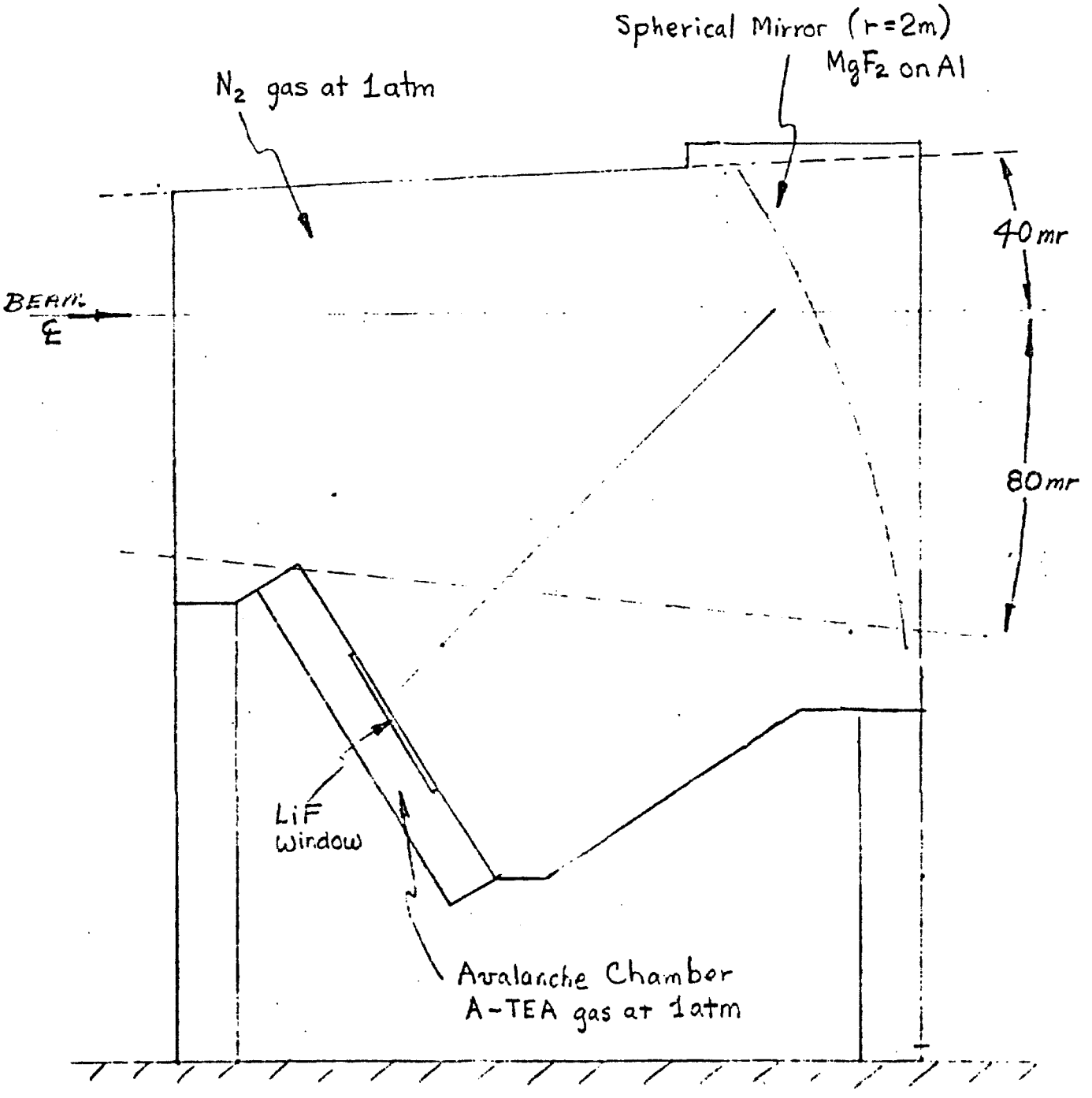

Fig. A2 Elevation View of Imaging Cerenkov Counter

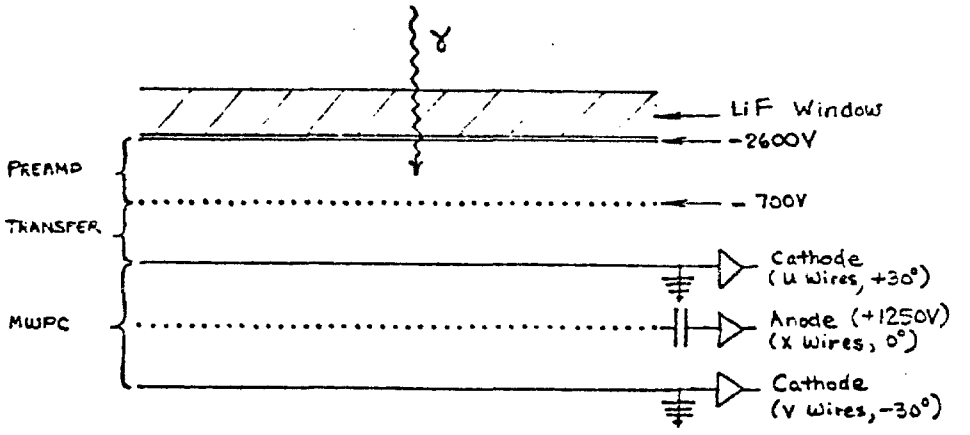

Fig. A3 Schematic of Avalanche Chamber. Wire spacing is 1.25 mm; interplane spacing is 3 mm.

Fig. A4: Portion of a quadrant of the liquid argon shower detector, indicating segmentation into an inner core of u,v readout strips and an outer portion of conventional x,y strips

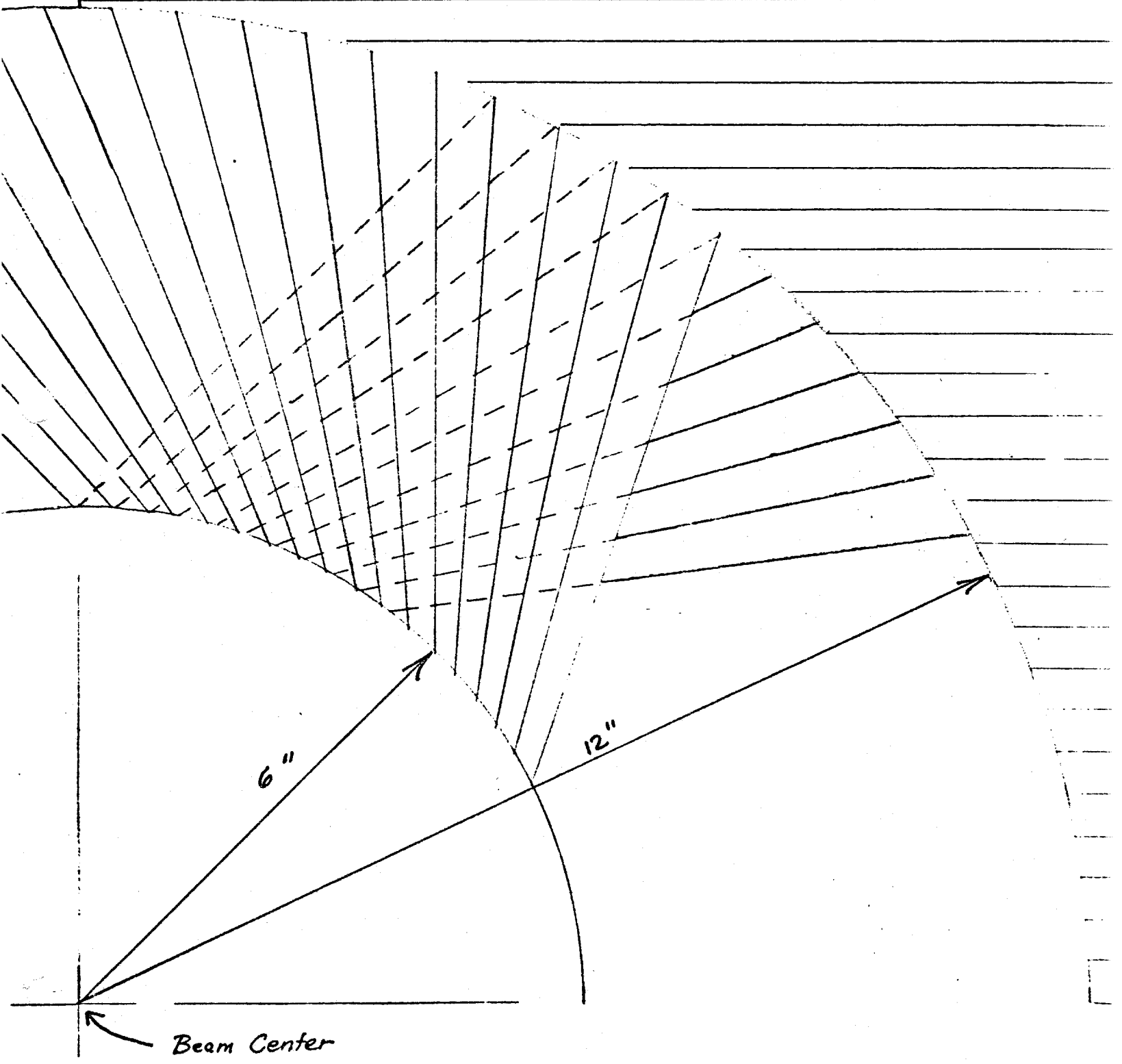

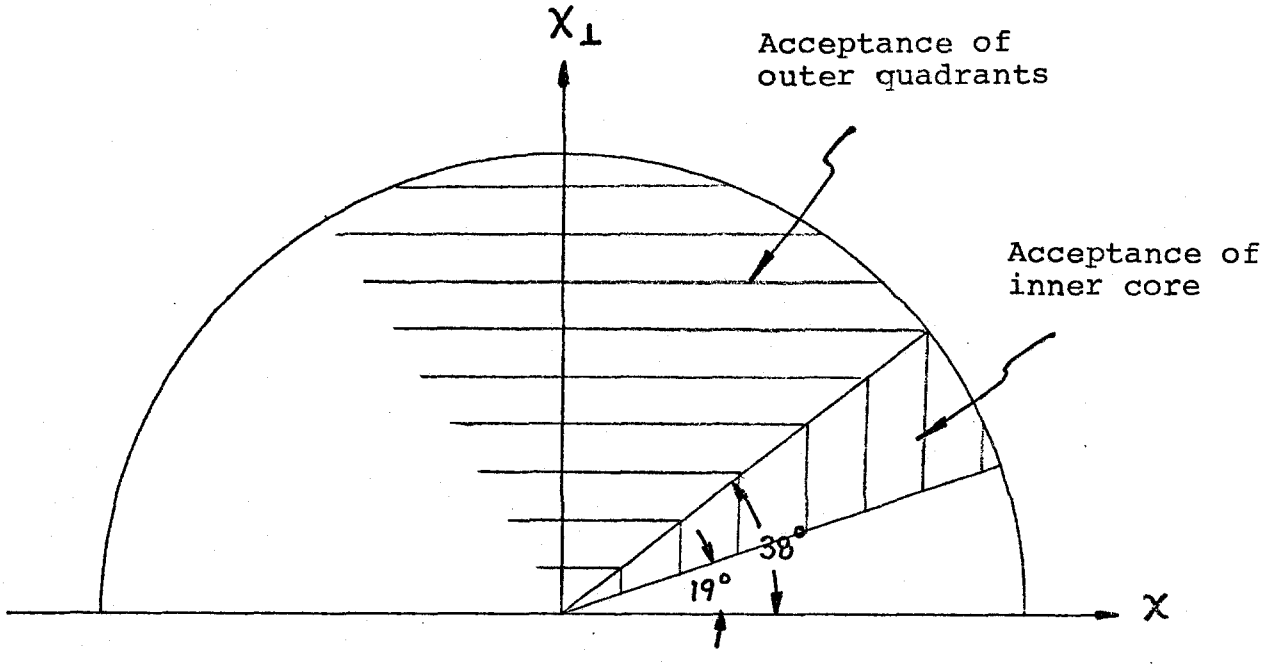

Fig. A5: Center-of-mass acceptance of the shower detector assuming $\sqrt{s}$ = 33.6 GeV (600 GeV beam of pions)

Appendix II:

Two New Triggerable Track Chamber - Targets

Douglas M. Potter
Serin Physics Laboratory
Rutgers University
Piscataway, New Jersey 08854

ABSTRACT

Two triggerable track chamber targets have been tested. A prototype scintillation camera has achieved a time resolution of 10 - 15 μs, a spatial resolution of about 30 μm (RMS) and a yield of 8 dots per mm of minimum ionizing track. A device containing a micro-channel plate target has achieved a spatial resolution of less than 10 μm and a yield of 2 dots per mm.

I. Introduction

Two devices have been investigated for possible use as triggerable track chamber - targets in experiments designed to search for short-lived particles and measure their lifetimes. Test results indicate that both devices should be valuable for such applications.

The first device is the scintillation camera, which is an improved version of the luminescent chamber of twenty years ago. The operating principle is through the use of an image intensifier to store, gate, and amplify and record on photographic film the image of a high energy interaction occurring in a scintillating target medium.

The second device is a microchannel plate (MCP). It has been found that a minimum ionizing particle passing through an MCP on a trajectory normal to the axes of the channels can excite a few per cent of the channels it traverses. An image can be formed and transferred to film in a manner similar to that used in the scintillation camera.

II. Scintillation Camera

The heart of the scintillation camera is a four stage magnetically focussed image intensifier (E.M.I. type 9912). As used in the scintillation camera, the first, third and fourth stages are quiescently on; the second stage is quiescently off. Scintillation light from an NaI(Tl) crystal target is focussed by a lens system onto the input photocathode of the image intensifier and stored on the first stage

phosphor for a length of time characteristic of the decay of the phosphor. When an interesting high energy interaction occurs in the target crystal the second stage of the image intensifier can be gated on (and the first off) to amplify the stored image further and transfer it to photographic film via another lens system. Some scintillation light not focussed onto the image intensifier is collected by a PMT, which is used in the formation of the event trigger (see Figure 1).

The images recorded on film are similar to those obtained with a bubble chamber or nuclear emulsion (see Figures 2 and 3). However, the scintillation camera is a triggerable device; those other two are not. Measured performance of a prototype scintillation camera and that expected of a practical device are summarized in Table 1. Measured results were obtained with a 7 GeV/c proton beam. Spatial resolution is limited in the prototype by the quality of the lens viewing the NaI(Tl) crystal and by reflections off the crystal backing; the ultimate limitations are diffraction in the viewing lens and depth of field required for a crystal of finite dimensions along the optical axis (i.e. parallel to the beam). Time resolution is governed primarily by the decay characteristics of the first stage phosphor, but is also affected by the characteristic curve of the film and the gate pulse length. The number of dots per mm. of track in the target is fixed by the lens aperture, efficiency of the scintillator, and absorption of the optical train. Dot size is determined primarily by the spatial resolution of the image intensifier.

III. Microchannel Plate

A microchannel plate (MCP) is a wafer of lead glass perforated by a matrix of tiny holes, or channels. Each channel acts as an independent electron multiplier, which can be excited by charged particles and UV, x- and γ- radiation. The probability of a channel to be excited by a charged particle depends on the secondary emission coefficient, and therefore on (among other things) the local specific ionization; consequently, the probability is small for a minimum ionizing particle.

To examine the feasibility of using an MCP as a triggerable track chamber - target, a proximity focussed MCP image intensifier tube was substituted for the NaI(Tl) crystal of the scintillation camera. The dimensions of the MCP were 18 mm diameter and .020" thick; the channels were 11 μm diameter and on 12.5 μm centers. A high energy beam was passed through the MCP parallel to the thin dimension (i.e. normal to the axes of the channels). Figures 4-6 and Table I display the results obtained with a 7 GeV/c proton beam. Note that the images are of nearly the same scale and look similar to those of the scintillation camera.

A practical device employing the MCP would look nothing like the apparatus used to test the feasibility of the technique. A thick MCP would be used both to increase the volume of the target and to produce by saturation dots of uniform intensity, and focussing would be via proximity throughout (i.e. gating would be accomplished by a proximity focussed diode image intensifier and fiber optic plates would be used for all optical coupling, including that to the film.)

Note that one would expect dots of smaller diameter; from the limiting resolution of the MCP image intensifier of about 25 lp/mm one would estimate a dot diameter of about 40-60 μm. It may be possible to find some new technique (as perhaps, collimation) to reduce the dot diameter to that of the channels.

TABLE I

PERFORMANCES OF SCINTILLATION CAMERA AND MCP DEVICE

	Dots/mm. of min. ionizing track	Dot Diameter (at Target)	Dot Resolution RMS (at Target)	Time Resolution	Target* Size
Measured performance of Prototype Scintillation Camera	8	20 μm	30 μm	10-15 μs	.015" x .375" x .375"
Expected performance of practical scintillation camera	8	20 μm	11 μm	<10 μs	.020" x .8" dia.
Measured performance of MCP test device	2	100-200 μm	<10 μm	Not Measured	.020" x .7" dia.
Expected Performance of practical MCP device	2	<60 μm	<10 μm	<10 μs	.1" x 2" dia.

*The first dimension listed is that along optical axis (transverse to beam).

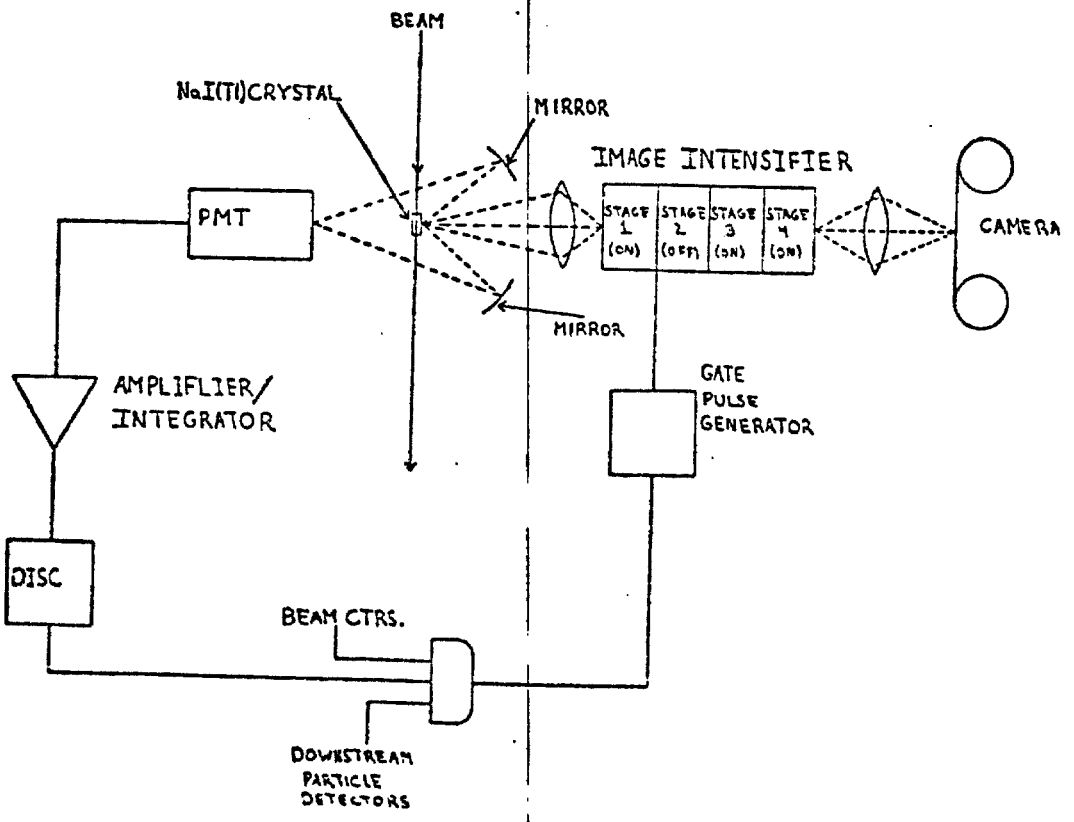

FIGURE I: Schematic of Scintillation Camera

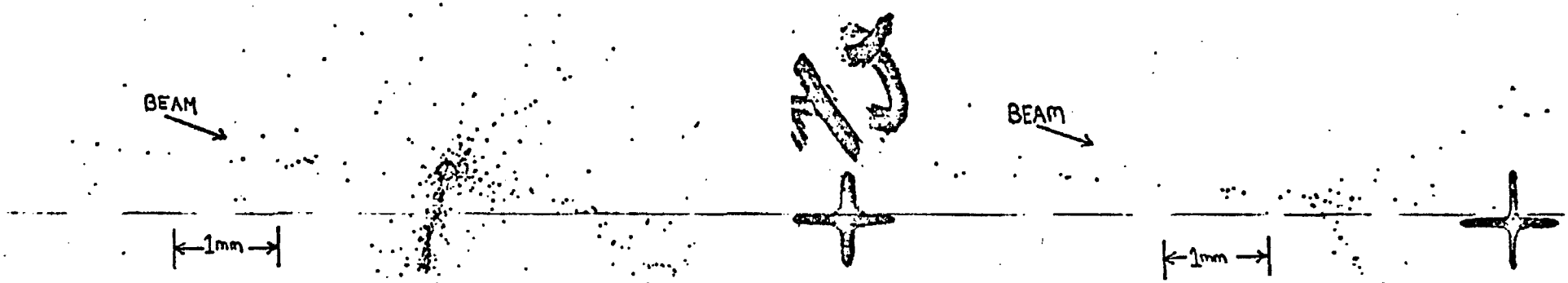

FIGURE II: A (typical) interaction in which nuclear breakup occurs recorded by the scintillation camera. (The reproduction in this and the following four figures do not do justice to the original images.)

FIGURE III: An (atypical) interaction in which no nuclear breakup occurs recorded by the scintillation camera.

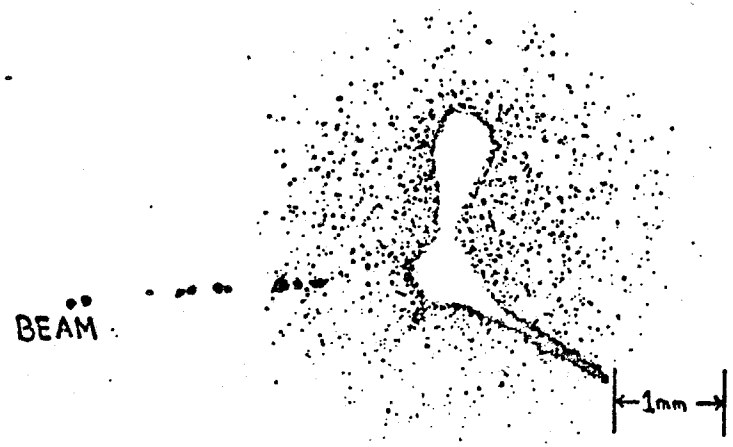

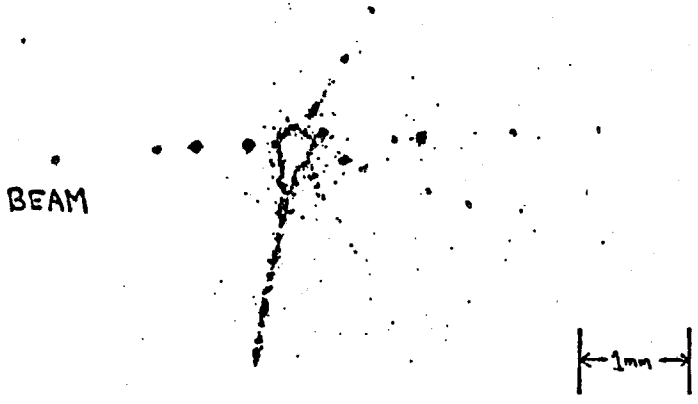

FIGURE IV: Two interactions recorded by the MCP device

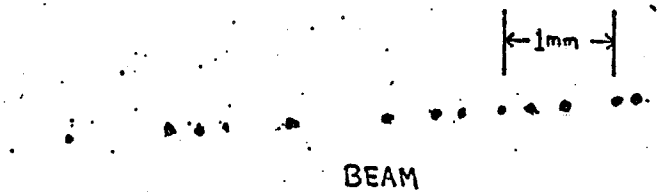

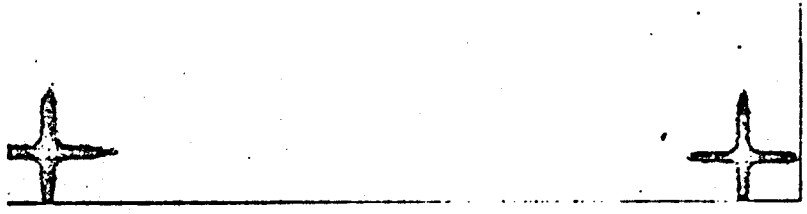

FIGURE V: Beam track recorded by the MCP device

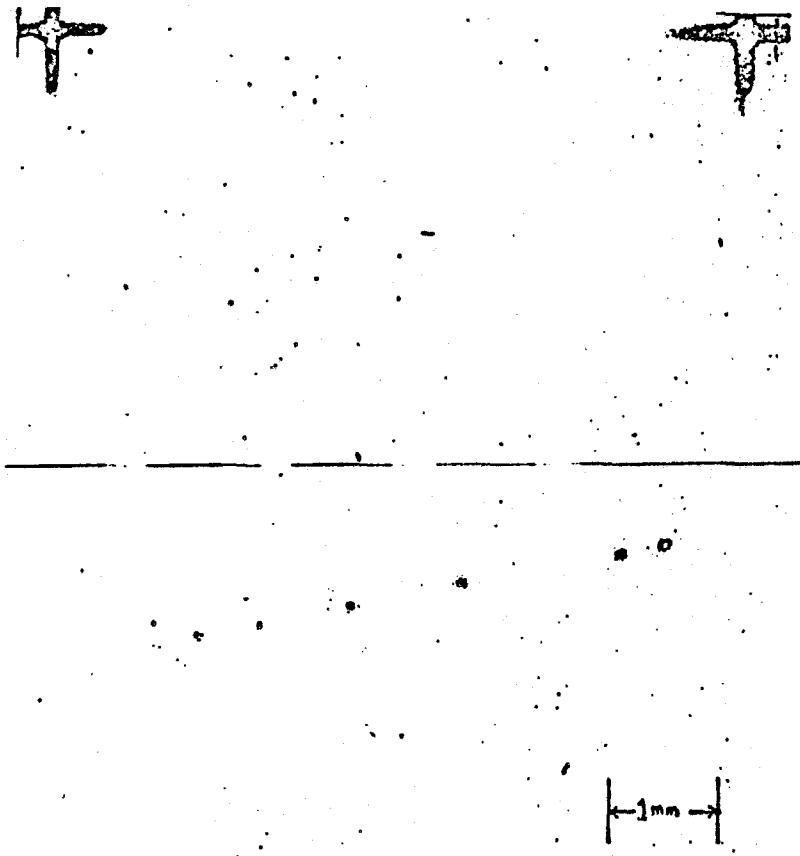

FIGURE VI: Track recorded by the MCP device. The photographic density of the individual dots is an indication of the local depth of the track in the MCP.